J Appl Electrochem (2008) 38:357–362
DOI 10.1007/s10800-007-9448-4

ORIGINAL PAPER

Effect of diffusion-layer porosity on the performance of polymer electrolyte fuel cells

G. Selvarani · A. K. Sahu · P. Sridhar · S. Pitchumani · A. K. Shukla

Received: 17 July 2007 / Revised: 1 November 2007 / Accepted: 2 November 2007 / Published online: 22 November 2007

Abstract The gas-diffusion layer (GDL) influences the performance of electrodes employed with polymer electrolyte fuel cells (PEFCs). A simple and effective method for incorporating a porous structure in the electrode GDL using sucrose as the pore former is reported. Optimal (50 w/o) incorporation of a pore former in the electrode GDL facilitates the access of the gaseous reactants to the catalyst sites and improves the fuel cell performance. Data obtained from permeability and porosity measurements, single-cell performance, and impedance spectroscopy suggest that an optimal porosity helps mitigating mass-polarization losses in the fuel cell resulting in a substantially enhanced performance.

Keywords Gas-diffusion layer · Mass transport · PEFC · Pore former · Porosity

1 Introduction

It is desirable for polymer electrolyte fuel cells (PEFCs) to operate at an optimal load current density for realizing highest possible power output both per total system size and weight. Advanced PEFCs utilize thin porous electrodes comprising macro porous (backing), micro porous (gas diffusion) and catalyst (reaction) layers. The gas diffusion layer (GDL) is positioned between macro-porous and catalyst layer, which consists of carbon black powder and some hydrophobic agent. The role of GDL in the PEFCs is to provide a proper pore structure to facilitate the accessibility of gaseous reactants to the catalyst sites while providing the path for the electrons to flow; GDL also plays an important role in the removal of reaction products from the catalyst layer [1–3]. The higher the operating current density of the fuel cell, the higher is the flux of the gas feed and an effective product removal from the reaction sites becomes imperative. This requires an ideal gas-diffusion layer to effectively transport reactant gases to the catalyst surface at optimum rate with concomitant removal of the product water from the catalytic sites.

Mass-transport effects, which contribute to loss in cell performance especially at higher load current densities, are: (i) water flooding wherein liquid water fills up the electrode pores creating a passive reaction-zone with consequent reduction in the effective electrode area and (ii) dilution of oxidant concentration due to the use of air instead of oxygen [4]. Mass-polarization losses could be mitigated by tailoring the porous electrode structure by an apt choice of materials properties and electrode composition in conjunction with the preparation method adopted for realizing the GDL [5].

Several studies have established the importance of GDL morphology in improving the cell performance [5–11]. The documented improvements relate to the PTFE content [6–8], the thickness of the diffusion layer [2] and the morphology of carbon black used [3, 9, 11] in the diffusion layer. However, studies on the influence of pore-size distribution in the GDL and its influence on the fuel cell performance are limited. Kong et al. [5] and Tucker et al. [10] have reported Li_2CO_3 as the pore-former in GDL for gas diffusion electrodes but the process for incorporation of

G. Selvarani · A. K. Sahu · P. Sridhar · S. Pitchumani · A. K. Shukla (✉)
Central Electrochemical Research Institute, Karaikudi 630 006, India
e-mail: shukla@sscu.iisc.ernet.in

A. K. Shukla
Solid State and Structural Chemistry Unit, Indian Institute of Science, Bangalore 560 012, India

pores in the GDL by the reported procedures is involved and a complete removal of Li-ions from the electrode needs to be ensured.

In this communication we report a simple and effective method for incorporating a porous structure in the GDL using sucrose as the pore-former. The optimum amount of the pore former in the GDL has been determined through cell impedance and polarization studies.

2 Experimental

2.1 Fabrication of membrane electrode assembly (MEA)

A Teflonised (15 w/o PTFE) carbon paper (Toray-TGP-H-120) of 0.37 mm thickness was employed as the backing layer. To prepare cathode GDL, the required amount of pore former (sucrose) and Vulcan-XC72R carbon was suspended in cyclohexane and agitated in an ultrasonic water bath for 30 min. To this, 15 w/o PTFE suspension was added with continuing agitation. The resultant slurry was spread onto a Teflonised carbon paper followed by copious washing with hot distilled water. Finally, the carbon slurry coated backing layer was sintered in air at 350 °C for 30 min. The anode-side GDL was prepared in a similar manner as mentioned but for the pore-former. Both anode and cathode diffusion layers contained 1.5 mg cm^{-2} of Vulcan XC-72R carbon (Cabot corp.), which was kept identical for all the electrodes.

To prepare reaction layer, the in-house prepared 40 w/o Pt catalyst supported onto Vulcan XC-72R carbon [12] was suspended in isopropyl alcohol. The mixture was agitated in an ultrasonic water bath and 7 w/o of Nafion (Dupont) solution was added to it with continuing agitation for 1 h. The resulting ink was coated onto the GDL. Both anode and cathode contain platinum loading of 0.5 mg cm^{-2} (active area 25 cm^2) that was kept identical for all the MEAs. To establish effective contact between the catalyst layer and the polymer electrolyte, a thin layer of Nafion solution diluted with isopropyl alcohol in 1:1 ratio was spread onto the surface of each electrode.

Nafion-1135 (DuPont) membrane was boiled with 30 v/o nitric acid for 1 h followed by its copious rinsing and washing with distilled water. It was then boiled in 5 v/o H_2O_2 for 1 h followed by copious washing with distilled water. Finally, the membrane was boiled in 1 M H_2SO_4 for 30 min followed by its repeated rinsing and washing in distilled water.

The membrane electrode assembly (MEA) was obtained by hot pressing the cathode and anode on either side of a pre-treated Nafion-1135 membrane at 25 kN ($\sim$60 kg cm^{-2}) at 130 °C for 3 min.

2.2 Electrochemical characterization

2.2.1 Design and polarization of PEFC single cells

MEAs were evaluated using a conventional 25 cm^2 fuel cell with parallel serpentine flow field machined on graphite plates (Schunk Kohlenstofftechnic). After equilibration, the single cells were tested at 60 °C with humidified gaseous hydrogen at a flow rate of 1 L per minute at anode and humidified gaseous oxygen at a flow rate of 1 L per minute at cathode at atmospheric pressure. While using air in place of oxygen, the flow rate was kept at 2.5 slpm. The polarization data on the PEFC were obtained using a fuel cell test station (model PEM-FCTS-158541) procured from Arbin Instruments, US.

2.2.2 Impedance measurements

An impedance analyzer (Autolab-PGSTAT 30) was employed to measure the resistance of the MEA at the operating cell voltage of 0.6 V. The reference and counter electrode leads were connected to the hydrogen electrode and the working electrode lead was linked to the oxygen electrode. Impedance measurements were conducted in the frequency range between 100 mHz and 5 kHz while imposing a sine wave of 10 mV amplitude.

2.3 Physical characterization of GDL

The surface morphology of cathode GDL were studied with the help of a JEOL JSM 5400 Scanning Electron microscope (SEM).

2.3.1 Porosity measurements

The porosity of each GDL was determined by the kerosene density (weighing) method [13]. In this technique, the sample was hanged and immersed in kerosene to fill all the pores. The bulk density (B_d) and the kerosene density (K_d) of the sample were measured with a Mettler balance (Model ME-40290) using Archimedes principle. The porosity was calculated by the following formula.

$$\text{Porosity} = \left(1 - \frac{B_d}{K_d}\right) \times 100\% \quad (1)$$

2.3.2 Gas permeability

Gas permeability coefficients for GDLs were obtained by using a home-built apparatus. The flow rate of nitrogen

across the GDL was controlled by a mass flow meter and the resultant pressure drop was measured by a manometer. Prior to measuring the through-plane permeability in the GDLs, they were pressed under identical conditions at which the MEAs are subjected to have proper evaluation of permeability. The cross sectional area of each sample was 25 cm^2. The permeability coefficient, which represents the gas permeability of a sample, was then calculated from Darcy's law [1, 5, 14].

$$V = \frac{K \times a \times \Delta P}{\mu \times l} \tag{2}$$

where V is the volumetric flow rate ($m^3\ s^{-1}$); K is Permeability (Darcy) coefficient (m^2); a is cross sectional area through which the flow passes (m^2); μ is gas viscosity (Pa s); l is the length of the conductive path (m); ΔP is the pressure drop across the sample (Pa).

3 Results and discussion

The surface morphology of a GDL (top-view) is shown in Fig. 1 as scanning electron micrographs at two different magnifications. Figure 1a and b shows the morphological features of GDL without pore former, while SEM photographs for GDLs with 25, 50 and 75 w/o of the pore-former, each with two magnifications, are shown in Fig. 1c–h. The difference in morphological features is noticed between GDLs without pore former and with varying content of the pore former, the latter revealing the formation of more pores with increasing pore-additive. Such an increase in porosity in GDLs may help increasing the oxygen transport and reduce water flooding in the electrode.

The porosity of each GDL and wet-proofed carbon paper are quantitatively depicted in Fig. 2. The porosity of TGP-H-120 carbon paper is found to be 78%, a value close to the specified value of 75.9%. The GDL shows 45% less porosity in relation to pristine Toray carbon paper suggesting that addition of a micro porous layer to the macro porous carbon paper decreases its porosity significantly. Furthermore, the percentage of porosity in GDL increases with increasing pore-former content.

Gas permeability is correlated to through pores, which serve as gas-transport paths in the fuel cell electrodes. A comparison of permeability coefficients for GDLs with and without pore-former is shown in Fig. 3. As expected, GDLs without pore former exhibit lesser permeability than those with pore former; the permeability increases with increasing pore-former content in the GDL. Williams et al. [15] have argued that at larger gas permeability in the GDL, gas transport occurs by diffusion with additional convection.

In order to understand the role of porosity in GDLs on the performance of PEFCs, especially at high load current densities, electrochemical impedance spectra ($Z = Z' + iZ''$) of H_2–Air cells were recorded at operating cell voltage of 0.6 V and the data are presented in Fig. 4. The high-frequency intercept with the real axis represents the ionic resistance of the electrolyte (R_s). The impedance spectrum at low frequencies shows polarization resistance (R_p), which is a combination of charge-transfer and diffusion resistances. Generally, diffusion resistance dominates the charge transfer resistance at high load current densities. At 0.6 V, the diameter of the semicircle decreases with increasing content of the pore former and the minimal value is observed with 50 w/o. The largest impedance loop is observed in the GDL without the pore-former. It could be articulated that increased porosity in GDL facilitates greater access of oxygen to the reaction sites decreasing the polarization resistance.

The performance of H_2–O_2 and H_2–Air PEFCs employing GDLs with 0, 25, 50 and 75 w/o of pore former have been evaluated from cell polarization data shown in Figs. 5 and 6. It can be seen that drop in cell voltage at high load current densities decreases with increasing content of the pore-former in the GDLs. The effect of GDL porosity is more pronounced for H_2–Air PEFCs as shown in Fig. 6. This could be owing to the lower partial pressure of oxygen in the air that results in the reduction of the effective reaction zone by nitrogen gas occupancy. Accordingly, the oxygen reduction reaction is rate limiting in the overall fuel cell reaction and results in a drastic drop, even at low load current densities. Furthermore, akin to the H_2–O_2 PEFC, the effect of water flooding is observed with exacerbated mass-transfer polarization in the porous electrode.

Among the H_2–O_2 and H_2–Air PEFC systems, the PEFC with electrodes comprising GDLs with pore former performs better in relation to the PEFC with electrodes comprising GDLs without the pore former over the entire polarization range. However, those with electrodes comprising GDLs with 50 w/o pore-former exhibit better performance than the PEFC with electrodes comprising GDLs with 75 w/o pore former. A higher amount of pore former in the GDL is expected to increase the utilization of platinum. However, this study suggests otherwise. This could be due to the decreased inter-carbon particles contact leading to an increased GDL resistance. Thus, the GDL with 50 w/o pore former is found to give maximum PEFC performance with optimum permeability for reactants in conjunction with minimum electrical resistance.

In both the H_2–O_2 and H_2–Air PEFC systems, the current density at operating cell voltage of 0.35 V is measured and the results are summarized in Table 1. The PEFC with electrodes comprising GDLs with pore former shows higher limiting current density compared to that with electrodes comprising GDLs without the pore former. The differences arise mainly from mass transport through GDL

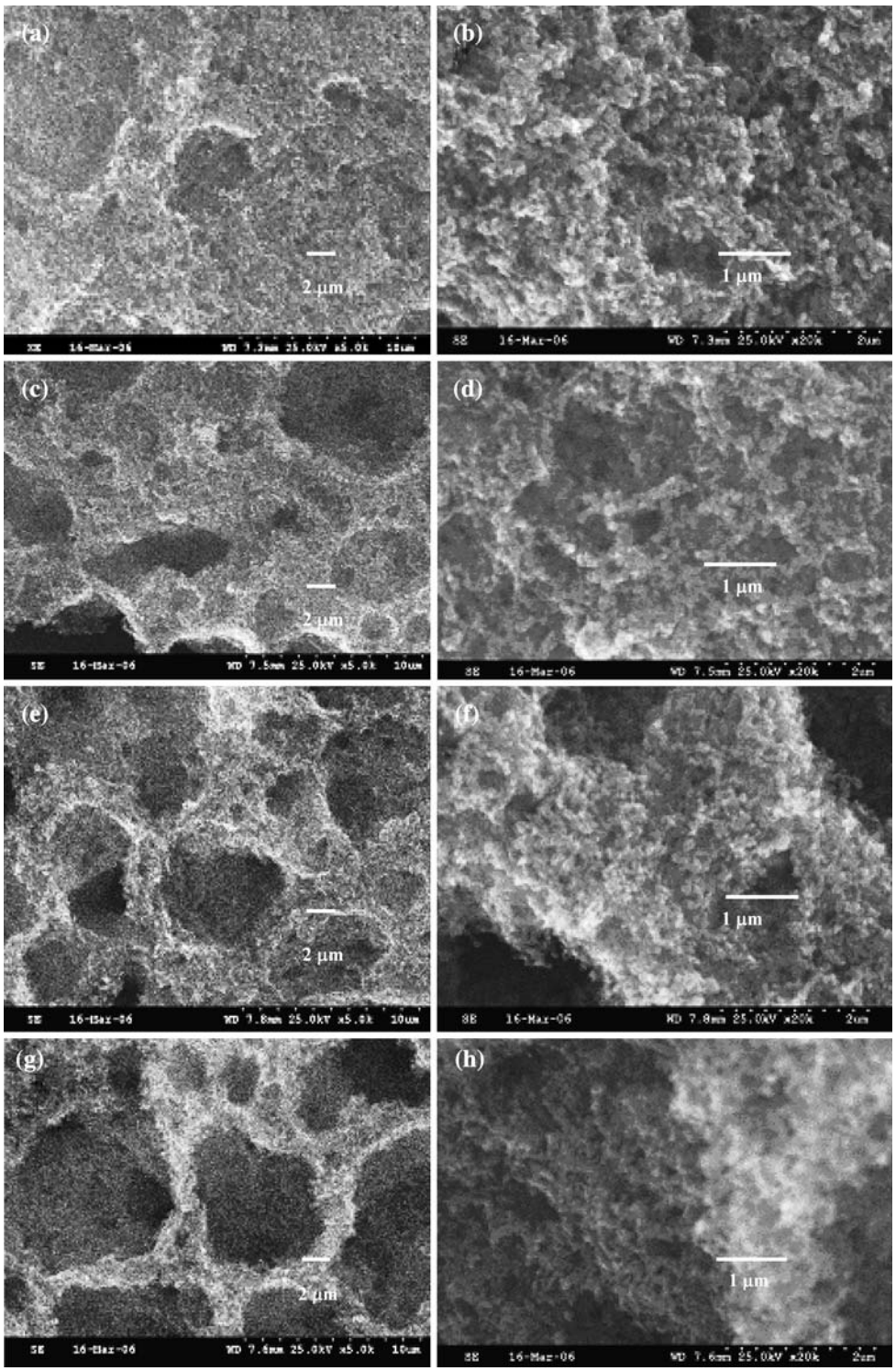

Fig. 1 SEM images for GDLs with (**c** and **d**) 25 w/o pore-former (**e** and **f**), 50 w/o pore former (**g** and **h**), 75 w/o pore former and without (**a** and **b**) pore former

as all the other factors are identical including catalyst loading, anode configuration, cell assembly, flow rate of reactant, pressure and operating condition. Moreover, the data indicate that the GDLs with 50 w/o pore-former show higher limiting current density in both H_2–O_2 and H_2–Air PEFC systems. Thus, these data corroborate the optimum content of pore former in the GDL to be 50 w/o.

The electrode kinetic parameters for the PEFCs are summarized in Table 2. The cell potential (E) versus current density (i) data at varying amounts of pore-former in GDLs are analyzed by fitting the data to equation,

$$E = E_0 - b \log i - iR \tag{3}$$

where $E_0 = E_r + b \log i_0$.

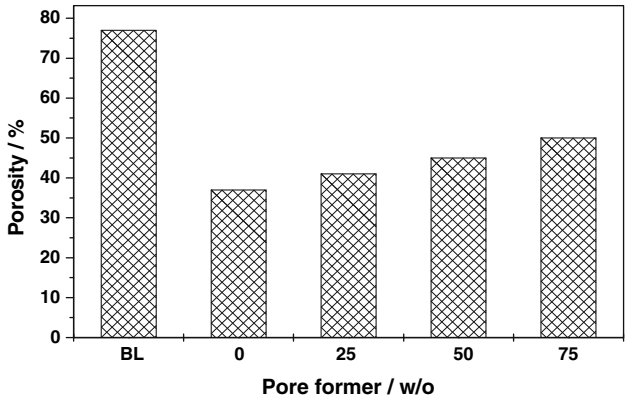

Fig. 2 Porosity of GDLs in the electrodes with and without pore former

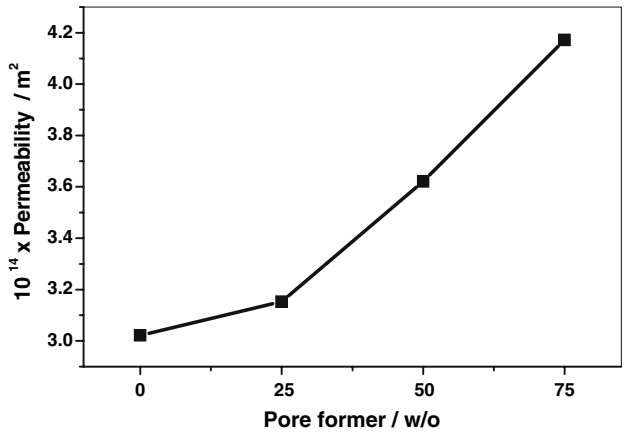

Fig. 3 Permeability of GDLs in the electrodes with varying pore-former content

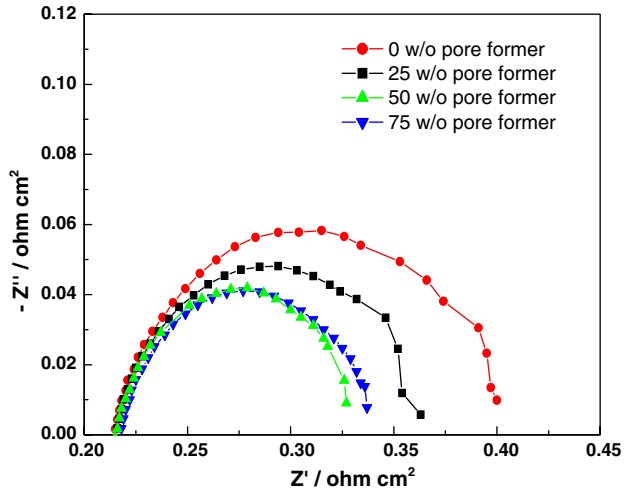

Fig. 4 Impedance spectra for PEFCs comprising GDLs with varying pore-former content at the operating cell voltage of 0.6 V

In Eq. 3, E_0 is the cell potential at a current density of 1 mA cm^{-2}; b is the Tafel slope, R accounts for the linear variation of overpotential with load current density primarily

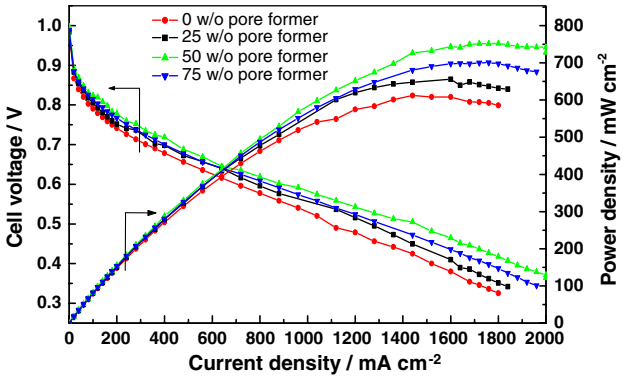

Fig. 5 Performance curves for PEFCs (H_2–O_2) comprising GDLs with and without pore former

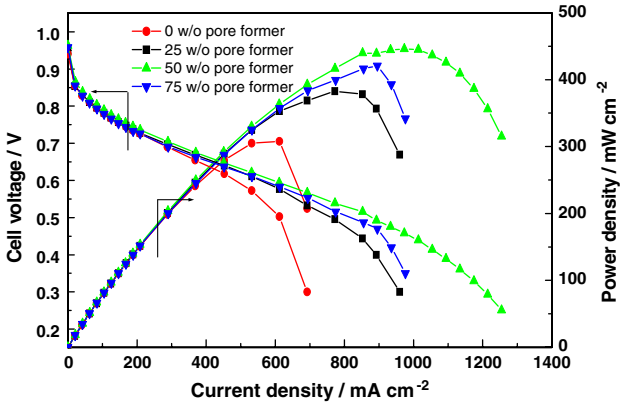

Fig. 6 Performance curves for PEFCs (H_2–Air) comprising GDLs with and without pore former

due to ohmic resistance. The value of $i_{0.9}$ represents the current density at the cell potential of 0.9 V. The reason for presenting $i_{0.9}$ and not i_0 is because even a slight variation in Tafel slope could vitiate the values of i_0 [12].

As seen from Table 2, the parameter R decreases with increasing pore-former content in the GDL for both H_2–O_2 and H_2–Air PEFC systems. R values are significantly higher for GDLs without pore-former compared to GDLs with pore former. This is a clear manifestation of the increased porosity in the GDLs so as to optimize the membrane electrode assembly resistance with enhanced three-phase interface. Accordingly, an increase in porosity facilitates high gas permeability to the catalyst layer. However, an increase in pore-former content to 75 w/o increases the resistance due to reduction of electronic conductivity of the GDL. The values of E_0 and $i_{0.9\ \mathrm{V}}$ exhibit similar trends with varying pore-former content in the GDL.

Tafel slopes from polarization curves for PEFCs with electrodes comprising GDLs with varying pore-former are lower than those with electrodes comprising GDLs without pore former. This could be due to the increased access of

Table 1 Effect of pore-former content on limiting-current density

w/o of pore-former in GDL	In oxygen current density at 0.35 V/A cm^{-2}	In air current density at 0.35 V/A cm^{-2}
0	1.7	0.672
25	1.801	0.927
50	2.08	1.149
75	1.94	0.987

Table 2 Electrochemical kinetic parameters for PEFCs with and without pore former in GDLs

w/o of pore-former in GDL	Oxidant	E_0/V	$i^{a}_{0.9}$/mA cm^{-2}	b/V decade^{1}	R/ohm cm^2
0	Oxygen	0.963	14.72	0.045	0.2136
	Air	0.959	9.12	0.073	0.4642
25	Oxygen	0.968	16.86	0.043	0.2062
	Air	0.963	10.35	0.065	0.4192
50	Oxygen	0.981	18.28	0.041	0.1734
	Air	0.973	13.42	0.059	0.3521
75	Oxygen	0.972	17.05	0.039	0.1895
	Air	0.969	11.60	0.063	0.3795

[a] $i_{0.9}$ is the current density at a cell potential of 0.9 V

the oxidant to the catalyst sites, which enhances the electrochemical performance of the cell. The kinetic data clearly show that the improved porosity in GDL not only increases the performance at higher load current densities but also helps reduce activation polarization, an observation also reported by Jordan et al. [2].

4 Conclusions

This study demonstrates the use of sucrose as a pore former in electrodes for PEFCs. The role of pore-former in mitigating mass-transfer resistance in PEFCs, especially at high load current densities, is illustrated employing porosity, permeability, impedance and polarization studies. Optimum pore-former content in the GDL of the gas-diffusion electrodes is important to optimize PEFC performance.

Acknowledgments This study was carried out under the New Millennium Indian Technology Leadership Initiative (NMITLI) program of Council of Scientific & Industrial Research (CSIR), New Delhi. We thank Dr. R. A. Mashelkar FRS for his constant encouragement and support. Selvarani is grateful to CSIR for a Senior Research Fellowship.

References

1. Mathias MF, Roth J, Fleming J, Lehnert W (2003) In: Veilstich W, Lamm A, Gasteiger HA (eds) Handbooks of fuel cells, vol 3. John Wiley, England, p 517
2. Jordan LR, Shukla AK, Behrsing T, Avery NR, Muddle BC, Forsyth M (2000) J Appl Electrochem 30:641
3. Jordan LR, Shukla AK, Behrsing T, Avery NR, Muddle BC, Forsyth M (2000) J Power Sources 86:250
4. Gostick JT, Fowler MW, Ionnidis MA, Pritzker MD, Volfkovich YM, Sakars A (2006) J Power Sources 156:375
5. Kong CS, Kim DY, Lee HY, Shul YG, Lee TH (2002) J Power Sources 108:185
6. Peganin VA, Ticianelli EA, Gonzalez ER (1996) J Appl Electrochem 26:297
7. Giorgi L, Antolini E, Pozio A, Passalacqua E (1998) Electrochim Acta 43:3675
8. Lim C, Wang CY (2004) Electrochim Acta 49:4149
9. Wang XL, Zhang HM, Zhang JL, Xu HF, Tian ZQ, Chen J, Zhong HX, Liang YM, Yi BL (2006) Electrochim Acta 51:4909
10. Tucker MC, Odgaard M, Lund PB, Andersen Y, Thomas JO (2005) J Electrochem Soc 152:A1844
11. Kannan AM, Munukutla L (2007) J Power Sources 167:330
12. Selvarani G, Sahu AK, Choudhury NA, Sridhar P, Pitchumani S, Shukla AK (2007) Electrochim Acta 52:4871
13. Mathur RB, Maheshwari PH, Dhami TL, Sharma RK, Sharma CP (2006) J Power Sources 161:790
14. Williams MV, Begg E, Bonville L, Kunz HR, Fenton JM (2004) J Electrochem Soc 151:A1173
15. Williams MV, Kunz HR, Fenton JM (2004) J Electrochem Soc 151:A1617